#63 Dupl

Experiment 63

FERMILAB-CONF-73-131-E

national accelerator laboratory °

PRODUCTION OF LARGE TRANSVERSE MOMENTUM GAMMA RAYS IN pp COLLISIONS FROM 50 TO 400 GeV

D. C. Carey, M. Goldberg*, J. R. Johnson, D. J. Ritchie, A. Roberts, R. Shafer, D. Theriot, E. von Goeler[†], J. K. Walker and M. Wong[††]

National Accelerator Laboratory
Batavia, Illinois

and

F. E. Taylor

Northern Illinois University
DeKalb, Illinois

Submitted to the IInd Aix-en-Provence International Conference on Elementary Particles, Aix-en-Provence, France
September 6 - 12, 1973

°Operated by Universities Research Association Inc. Under Contract with the United States Atomic Energy Commission

ABSTRACT

We have measured the single photon inclusive cross section, $d\sigma_\gamma/dkd\Omega$ for the reaction $p + p \rightarrow \gamma$ + anything for incident proton energies between 50 GeV and 400 GeV and at a fixed angle of 100 mrads in the laboratory. This can be related to the invariant π° cross section. The results indicate that the invariant π° cross section falls exponentially, as a function of transverse momentum, for an incident proton energy of 50 GeV. At higher incident momenta there is a deviation from a simple exponential at transverse momenta greater than about 1 GeV/c. Preliminary results are given on the energy dependence of this deviation.

APPARATUS AND DATA ACQUISITION

This experiment was performed using an internal target in the CO straight section of the National Accelerator. Data were taken over the complete range of proton energy available during the acceleration cycle.

The target was either a hydrogen gas jet [1,2] or a rotating carbon fiber target. The data presented here were obtained for both targets at a fixed laboratory angle of 100 mrad for the detected gamma ray. A lead collimator restricted the apparatus to detecting only one of the two photons from a π° decay.

The schematic of the apparatus is shown in Figure 1. The distance to the target was 16.46m and the solid angle acceptance was 9.5 μster. The lead converter was 1.1 radiation lengths thick and the lead-glass total-absorption counter had an effective length of 14 radiation lengths.

An energy calibration of the lead-glass Cerenkov counter 4 was made using 1.8 to 5 GeV/c electrons and muons at Argonne National Laboratory. The photomultiplier and base were tested and found to be linear up to a response equivalent to 280 GeV photon energy. The response of the counter to muons (defined by a 1·2·3·5·6 trigger) was monitored during data taking. The pulse height distribution from counter 4 for this trigger showed a clean peak with a 30% FWHM. The muon peak provided a calibration check during the runs.

The photon data was taken using a $\overline{1}\cdot 2\cdot 3\cdot 4$ trigger. When a trigger occurred, the pulse heights in all counters, the main ring magnetic field (which gave the proton incident momentum) and other scaler information were written onto magnetic tape for later analysis. Data were taken both with the converter in and the converter out. The converter-out data rate was less than 1.5% of the converter-in rate. Furthermore, the converter-out spectra were parallel to the converter-in spectra to the highest transverse momenta. This behavior was consistent with photon conversion in the counters themselves and no correction was made for converter-out background.

PRELIMINARY ANALYSIS AND RESULTS

The photon data were divided into 25 GeV bins in the incident proton energy. For the gas-jet target only those bins actually containing events from the jet were used in further analysis. A cut on the pulse height in trigger counter 2 required that events have a doubly ionizing or greater pulse height in that counter.

Examples of the energy spectra of the lead-glass counter are shown in Figures 2 and 3 for 50 GeV and 375 GeV incident proton energy. The observed photon spectra were fitted with a function of the form

$$\frac{d\sigma_\gamma}{dk\,d\Omega} = Ae^{-Bp_\perp} \qquad (1)$$

where A and B are free parameters. The results of this procedure for the hydrogen data are shown in Table I. With the exception of the 50 GeV data, these fits did not give acceptable χ^2. A second function was tried of the form

$$\frac{d\sigma_\gamma}{dk\,d\Omega} = Ae^{-Bp_\perp - Cp_\perp^2} \qquad (2)$$

where A, B, and C are free parameters. Acceptable fits to the data were obtained in all cases. The results are shown in Table II. All errors given are statistical. Systematic errors have not yet been included.[3]

The same function was then used to fit the carbon data. The results for carbon are shown in Table III. As can be seen there is good agreement between the parameters obtained for the hydrogen and carbon data.

The invariant π° cross section can be derived from the inclusive photon spectrum by means of the usual Sternheimer analysis[4]

$$E\frac{d\sigma\pi}{d^3p} \propto \frac{\partial}{\partial k}\frac{d\sigma_\gamma}{dkd\Omega} \qquad (3)$$

using equation (2) and (3) we obtain

$$E\frac{d\sigma\pi}{d^3p} = \tilde{A}(B+2Cp_\perp)\left(\frac{d\sigma_\gamma}{dkd\Omega}\right)_{data} \qquad (4)$$

where $\tilde{A}$ is a normalization factor. Using the parameters B and C from the fits to the photon spectrum we can thus derive an invariant $\pi°$ cross section spectrum. This procedure was termed the pseudo-derivative method. Examples of the results of such a procedure are shown in Figures 4 and 5. The 50 GeV data in Figure 2 were adequately fitted by a single exponential (i.e. C = 0). Therefore the derived $\pi°$ spectrum in Figure 4 has the same shape as the photon spectrum. The 375 GeV data shown in Figure 3 had a non-zero C. Therefore, this procedure changes the shape slightly, suppressing the high $p_\perp$ values since our fitter C is negative.

The derived $\pi°$ invariant cross-sections were then fitted to the function $Ae^{-Bp_\perp-Cp_\perp^2}$, with A, B, and C as free parameters. The results are given in Tables IV and V.

DISCUSSION OF RESULTS

In Figures 6 and 7 we present plots of the values of the parameters B and C versus incident proton energy for the gamma spectra from the hydrogen and carbon targets. We find agreement between the two targets for the parameters. The data given here represent all of the hydrogen data taken at this angle, but only about 25% of the carbon data. The data seem to require a B parameter that does not vary significantly with energy. On the other hand, the C parameter starts out at zero, increases sharply between 50 and 125 GeV, then is approximately independent of incident proton energy. This C parameter effectively measures the deviation from simple exponential behavior.

It should be emphasized that our experiment is performed at fixed laboratory angle and that there is a relation between $p_\perp$ and x (where $x=p^*_{||}/p_{max}^*$). For example at 100 mrad laboratory angle and 50 GeV, a $p_\perp$ of 2.3 GeV/c corresponds to an x of 0.4 while at 200 GeV all values of $p_\perp$ correspond closely to x=0. Furthermore, the data taken at high $p_\perp$ for the lower energies lie closer to the kinematic boundary than those taken at higher energies. Thus these effects may very well be responsible for the behavior of the C parameters. At this time we are making measurements at different laboratory angles to study these effects.

Results are given in Figures 8 and 9 for the fits to the invariant π° spectra. These plots show the same general features discussed in connection with Figures 6 and 7. The values of C for the π° spectra are in good agreement with those found at the ISR[5] for charged pions in the energy region where overlap occurs.

In conclusion, we confirm the results from the ISR[5,6] that the single particle inclusive distribution deviates markedly from a simple exponential behavior. In addition, we have obtained preliminary results that show the energy dependence of this deviation between 50 GeV and 400 GeV.

The authors wish to thank E. Malamud, D. Jovanovic, and the staff of the Internal Target Laboratory for their help in making this experiment possible. We are indebted to the members of the USSR-USA collaboration for providing us with the opportunity to use the hydrogen-jet target, and we would especially like to thank V. Bartenev, A. Kuznetsov, B. Morosov, V. Nikitin, Y. Pilipenko, V. Popov, and L. Zolin, the visiting Soviet scientists. We should also like to acknowledge the help of the synchroton operating staff for providing us with a 400 GeV beam. The assistance of our technicians, D. Burandt and R. Olsen, is gratefully acknowledged.

---

* Visiting scientist, permanent address: University of Paris, Paris, France.

† Visiting scientist, permanent address: Northeastern University, Boston, Massachusetts.

†† Visiting scientist, permanent address: Princeton University, Princeton, New Jersey.

REFERENCES

[1]Development and Operation of Hydrogen Jet Target Supported by The State Committee for Utilization of Atomic Energy of The USSR, Moscow.

[2]V. Bartenev, et. al., Phys. Rev. Lett. 29, 1755 (1972).

[3]At the present time we quote a ±10% energy calibration of the lead glass counter.

[4]R. M. Sternheimer, Phys. Rev. 99, 277 (1955).

[5]M. Banner, et. al., Phys. Lett. 41B, 547 (1972; Phys. Lett. 537 (1973).

[6]B. Alper, et. al., Phys. Lett. 44B, 521 (1973).

Table I Parameters for Fits of the Form $Ae^{-Bp_\perp}$ To Gamma Spectra From the Hydrogen Jet Target

E_p (GeV)	$p_{\perp max}$ (GeV/c)	B $(GeV/c)^{-1}$	C $(GeV/c)^{-2}$	χ^2 Per Degree of Freedom
50	2.26	5.51 ± .01	-	0.78
75	-	-	-	-
100	2.91	5.02 ± .03	-	5.35
125	2.48	5.23 ± .03	-	1.87
150	-	-	-	-
175	3.50	4.54 ± .03	-	1.15
200	2.95	4.94 ± .03	-	2.82
225	-	-	-	-
250	3.10	4.66 ± .03	-	4.50
275	2.98	4.77 ± .04	-	7.05
300	-	-	-	-
325	-	-	-	-
350	-	-	-	-
375	2.88	4.86 ± .04	-	5.05
400	-	-	-	-

Table II Parameters for Fits of the Form $Ae^{-Bp_\perp - cp_\perp^2}$ For Gamma Spectra From the Hydrogen Jet Target

E_p (GeV)	$p_{\perp max}$ (GeV/c)	B $(GeV/c)^{-1}$	C $(GeV/c)^{-2}$	χ^2 Per Degree of Freedom
50	2.26	5.52 ± .03	-.009 ± .020	.79
75	-	-	-	-
100	2.91	5.64 ± .04	-.343 ± .020	1.38
125	2.48	5.78 ± .06	-.366 ± .033	.78
150	-	-	-	-
175	3.50	5.54 ± .12	-.306 ± .036	.68
200	2.95	5.69 ± .05	-.403 ± .022	.76
225	-	-	-	-
250	3.10	5.40 ± .06	-.387 ± .025	1.51
275	2.98	5.62 ± .05	-.489 ± .024	1.62
300	-	-	-	-
325	-	-	-	-
350	3.07	5.62 ± .23	-.474 ± .066	1.18
375	2.88	5.75 ± .05	-.513 ± .023	1.06
400	-	-	-	-

Table III Parameters For Fits of the Form $Ae^{-Bp_\perp - cp_\perp^2}$ For Gamma Spectra From the Carbon Fiber Target

E_p (GeV)	$p_{\perp max}$ (GeV/c)	B $(GeV/c)^{-1}$	C $(GeV/c)^{-2}$	χ^2 Per Degree of Freedom
50	2.36	5.41 ± .08	+.106 ± .040	.48
75	2.79	5.61 ± .07	-.193 ± .031	.53
100	2.95	5.69 ± .09	-.164 ± .040	.95
125	2.95	5.66 ± .08	-.378 ± .032	.88
150	3.10	5.41 ± .06	-.321 ± .027	.67
175	2.95	5.45 ± .07	-.342 ± .029	.81
200	3.13	5.51 ± .06	-.370 ± .026	.68
225	3.07	5.76 ± .07	-.416 ± .029	.77
250	3.85	5.68 ± .07	-.500 ± .028	.72
275	3.13	5.56 ± .07	-.471 ± .028	.91
300	3.07	5.62 ± .06	-.423 ± .028	.77
325	2.76	5.68 ± .06	-.488 ± .029	.73
350	2.79	5.52 ± .08	-.392 ± .039	.93
375	2.95	5.48 ± .07	-.435 ± .029	1.08
400	3.04	5.44 ± .07	-.339 ± .033	1.00

Table IV Parameters For Fits of the Form $Ae^{-Bp_\perp - cp_\perp^2}$
For the "π°" Spectra From the Gas Jet Target

E_p (GeV)	$p_\perp$ max (GeV/c)	B $(\text{GeV}/c)^{-1}$	C $(\text{GeV}/c)^{-2}$	χ^2 Per Degree of Freedom
50	2.26	5.51 ± .03	-.005 ± .020	.70
75	-	-	-	-
100	2.91	5.74 ± .04	-.325 ± .020	1.27
125	2.48	5.91 ± .06	-.355 ± .033	.72
150	-	-	-	-
175	3.50	5.69 ± .13	-.310 ± .036	.54
200	2.95	5.83 ± .05	-.390 ± .022	.73
225	-	-	-	-
250	3.10	5.52 ± .06	-.365 ± .025	1.43
275	2.98	5.76 ± .05	-.452 ± .024	1.47
300	-	-	-	-
325	-	-	-	-
350	3.07	5.57 ± .26	-.393 ± .072	.88
375	2.88	5.91 ± .05	-.482 ± .023	.94
400	-	-	-	-

Table V Parameters For Fits of the Form $Ae^{-Bp_\perp - cp_\perp^2}$ For The "π°" Spectra From the Carbon Fiber Target

E_p (GeV)	$p_\perp$ max (GeV/c)	B $(GeV/c)^{-1}$	C $(GeV/c)^{-2}$	χ^2 Per Degree of Freedom
50	2.34	5.37 ± .08	+.109 ± .040	.46
75	2.79	5.68 ± .07	-.189 ± .031	.51
100	2.95	5.74 ± .09	-.160 ± .040	.92
125	2.95	5.78 ± .08	-.361 ± .033	.87
150	3.1	5.52 ± .06	-.309 ± .027	.65
175	2.95	5.56 ± .07	-.327 ± .029	.79
200	3.13	5.64 ± .06	-.353 ± .026	.67
225	3.07	5.89 ± .07	-.399 ± .029	.75
250	2.85	5.84 ± .07	-.471 ± .028	.70
275	3.13	5.70 ± .07	-.441 ± .028	.88
300	3.07	5.76 ± .07	-.403 ± .028	.76
325	2.76	5.84 ± .07	-.461 ± .029	.71
350	2.79	5.62 ± .08	-.362 ± .039	.86
375	2.95	5.62 ± .07	-.408 ± .029	1.04
400	3.04	5.56 ± .07	-.326 ± .033	.96

FIGURE CAPTIONS

Figure 1 Schematic of the apparatus.

Figure 2 Single photon inclusive cross section $d\sigma_\gamma/dkd\Omega$ for the reaction $p + p \to \gamma$ + anything for incident proton energy of 50 GeV

Figure 3 Single photon inclusive cross section $d\sigma_\gamma/dkd\Omega$ for the reaction $p + p \to \gamma$ + anything for incident proton energy of 375 GeV.

Figure 4 Derived invariant π° cross section $E\frac{d\sigma}{d^3p}$ for the reaction $p + p \to \gamma$ + anything for incident proton energy of 50 GeV.

Figure 5 Derived invariant π° cross section $E\frac{d\sigma}{d^3p}$ for the reaction $p + p \to \gamma$ + anything for incident proton energy of 375 GeV

Figure 6 Values of the parameters B and C for the photon inclusive cross sections from the hydrogen jet target for proton energies between 50 and 375 GeV

Figure 7 Values of the parameters B and C for the photon inclusive cross sections from the carbon fiber target for proton energies between 50 and 400 GeV

Figure 8 Values of the parameters B and C for the derived invariant π° cross sections from the hydrogen jet target for proton energies between 50 and 375 GeV

Figure 9 Values of the parameters B and C for the derived invariant π° cross sections from the carbon fiber target for proton energies between 50 and 400 GeV

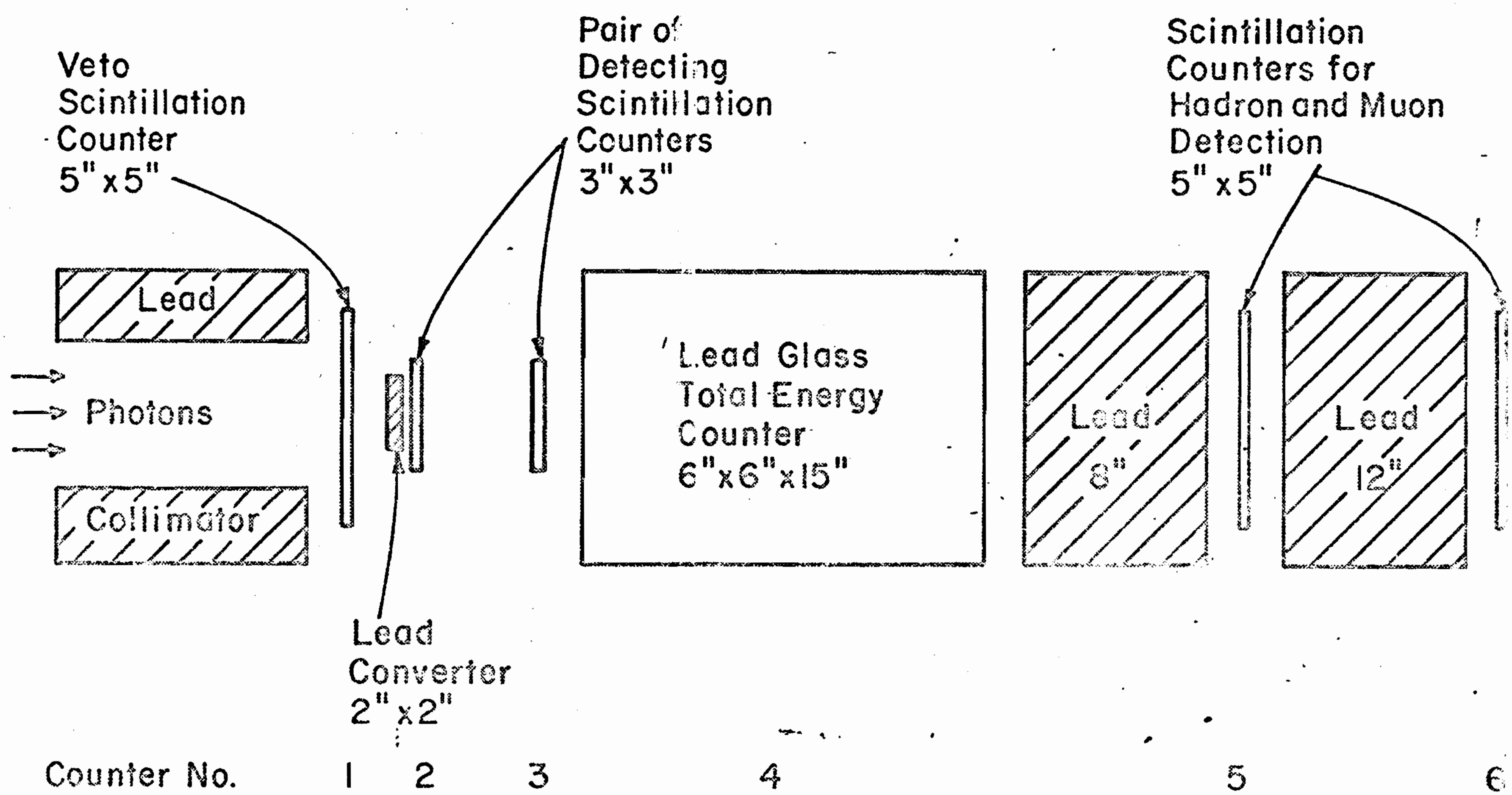

Veto Scintillation Counter 5"x5"
Pair of Detecting Scintillation Counters 3"x3"
Scintillation Counters for Hadron and Muon Detection 5"x5"
Lead
Photons
Collimator
Lead Glass Total Energy Counter 6"x6"x15"
Lead 8"
Lead 12"
Lead Converter 2"x2"
Counter No. 1 2 3 4 5 6

FIGURE 1

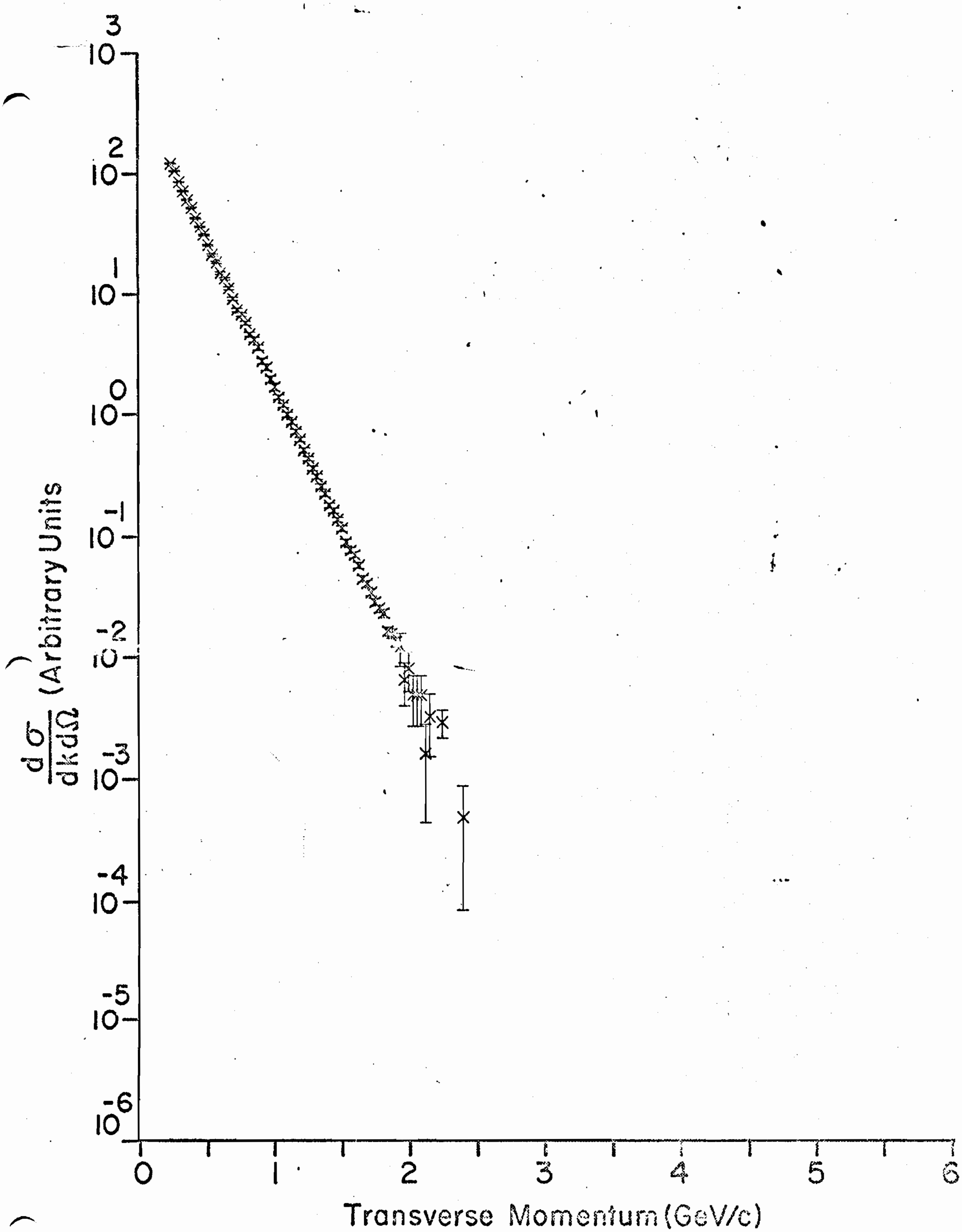

$\frac{d\sigma}{dk\,d\Omega}$ (Arbitrary Units)
10^{3}
10^{2}
10^{1}
10^{0}
10^{-1}
10^{-2}
10^{-3}
10^{-4}
10^{-5}
10^{-6}
0
1
2
3
4
5
6
Transverse Momentum (GeV/c)

FIGURE 2

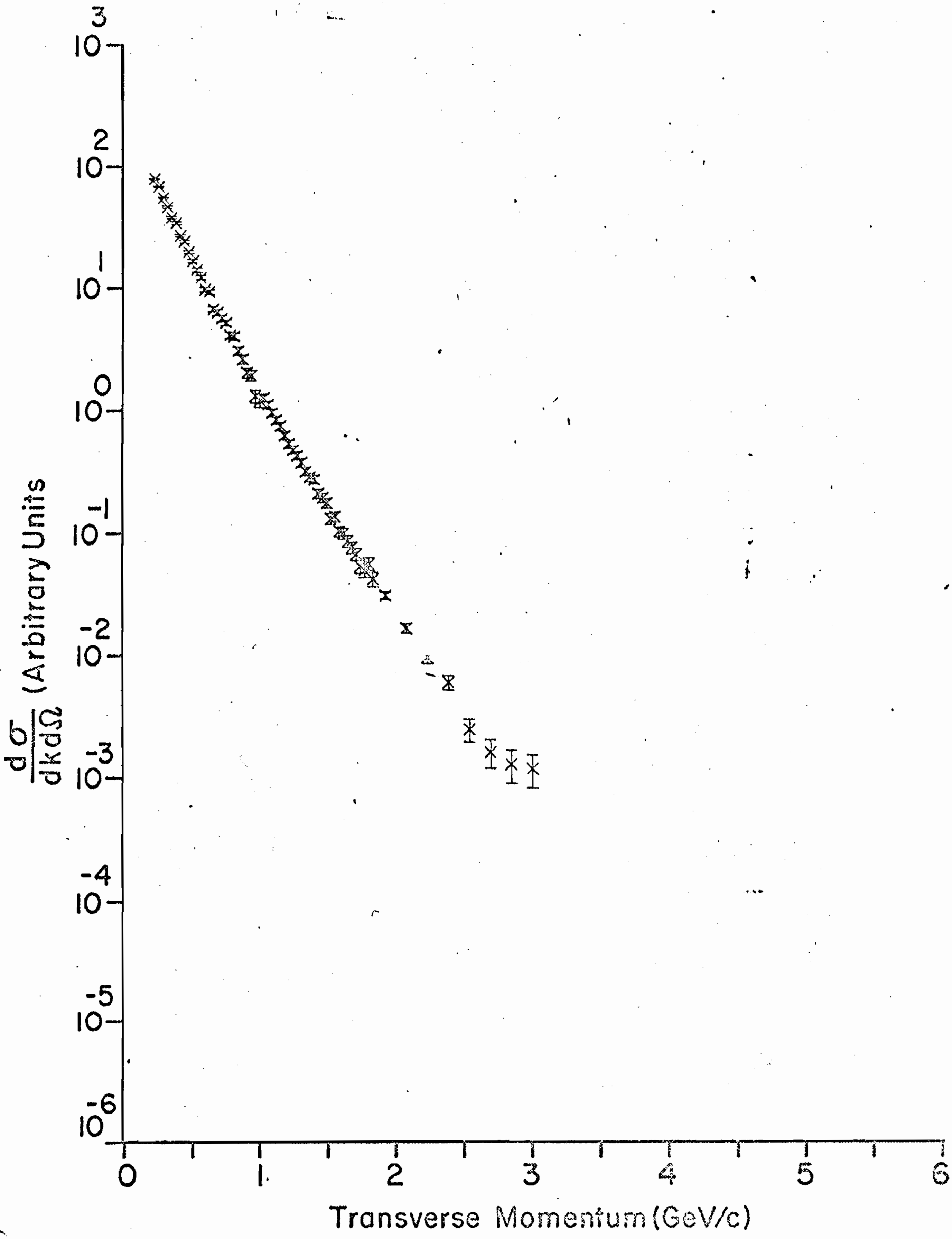
$\frac{d\sigma}{dk\,d\Omega}$ (Arbitrary Units)
10^{3}
10^{2}
10^{1}
10^{0}
10^{-1}
10^{-2}
10^{-3}
10^{-4}
10^{-5}
10^{-6}
0
1
2
3
4
5
6
Transverse Momentum (GeV/c)

FIGURE 3

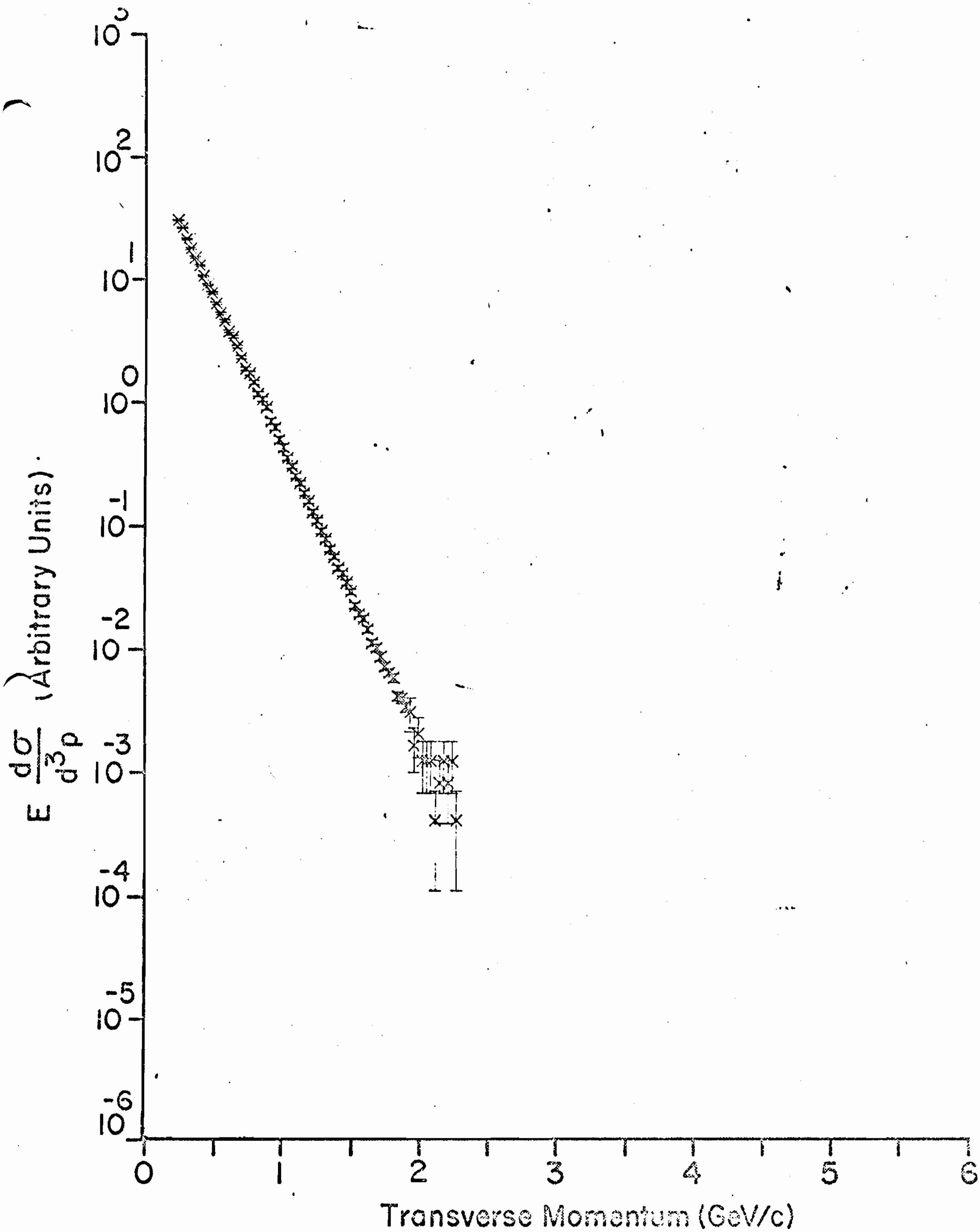

10^3
10^2
10^1
10^0
10^-1
10^-2
10^-3
10^-4
10^-5
10^-6
E dσ/d³p (Arbitrary Units)
0
1
2
3
4
5
6
Transverse Momentum (GeV/c)

FIGURE 4

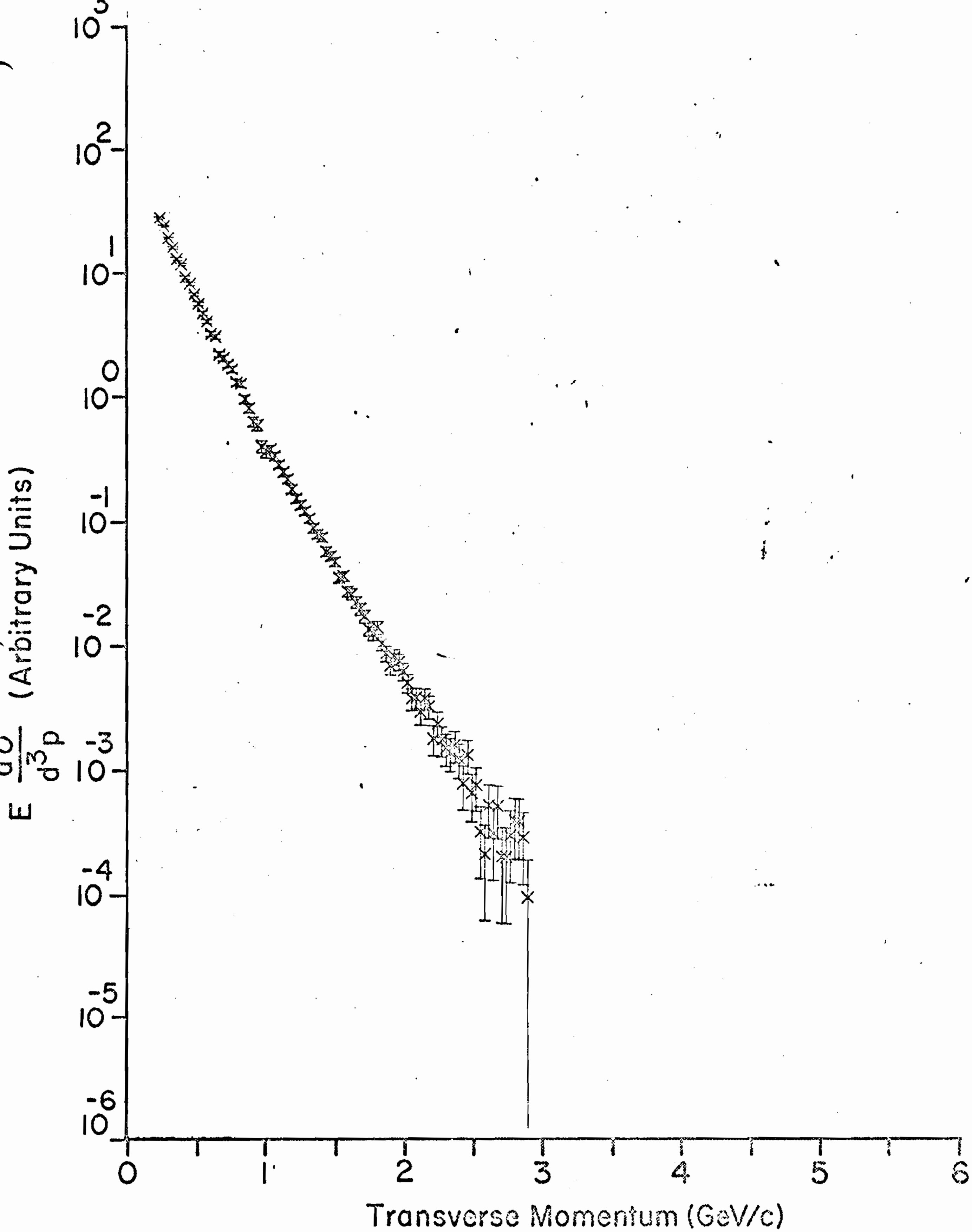

10^{3}
10^{2}
10^{1}
10^{0}
10^{-1}
10^{-2}
10^{-3}
10^{-4}
10^{-5}
10^{-6}
$E \frac{d\sigma}{d^3p}$ (Arbitrary Units)
0
1
2
3
4
5
6
Transverse Momentum (GeV/c)

FIGURE 5

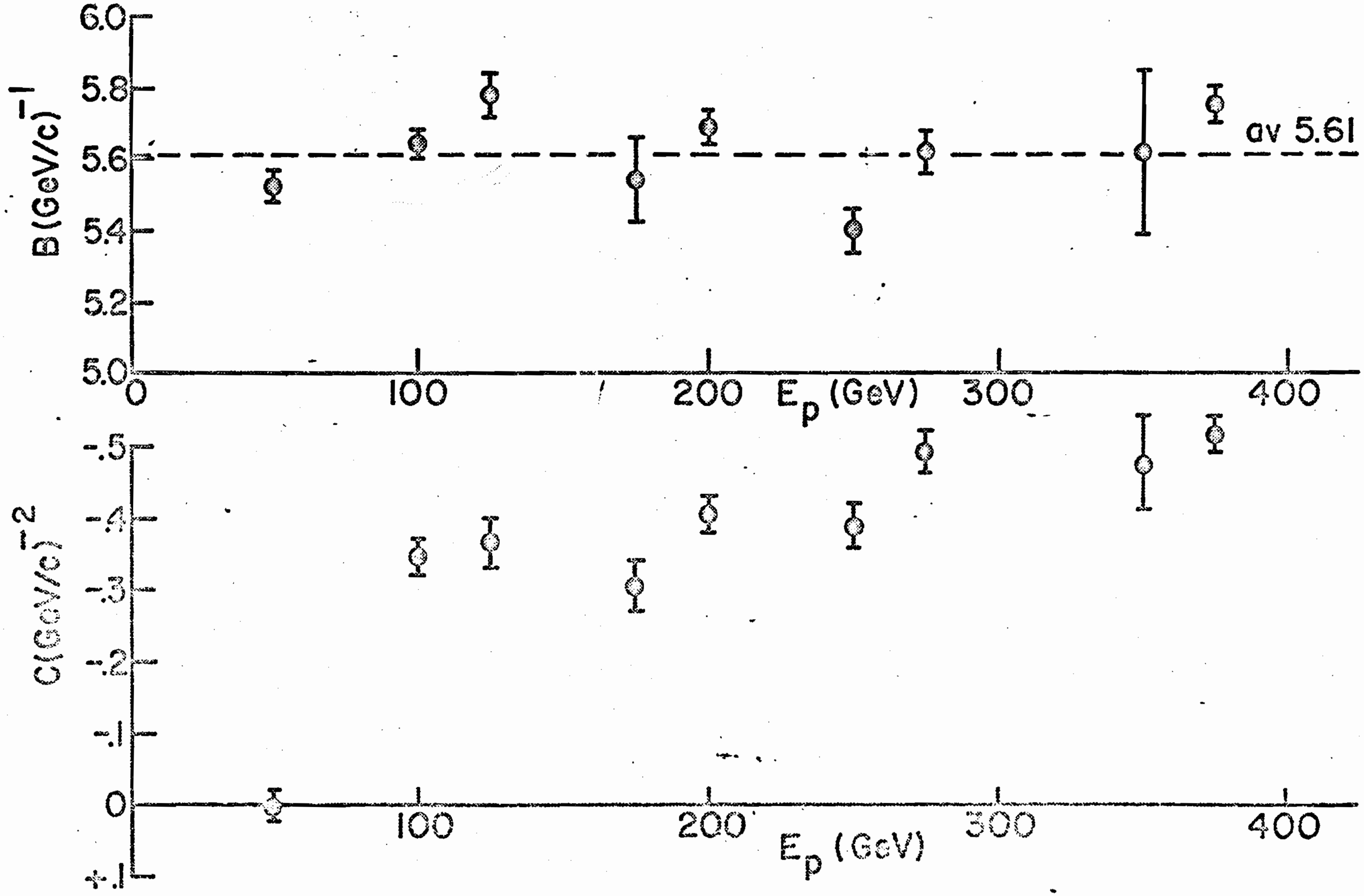

6.0
5.8
5.6
5.4
5.2
5.0
B(GeV/c)$^{-1}$
av 5.61
0
100
200
300
400
E_p (GeV)
-.5
-.4
-.3
-.2
-.1
0
+.1
C(GeV/c)$^{-2}$
100
200
300
400
E_p (GeV)

FIGURE 6

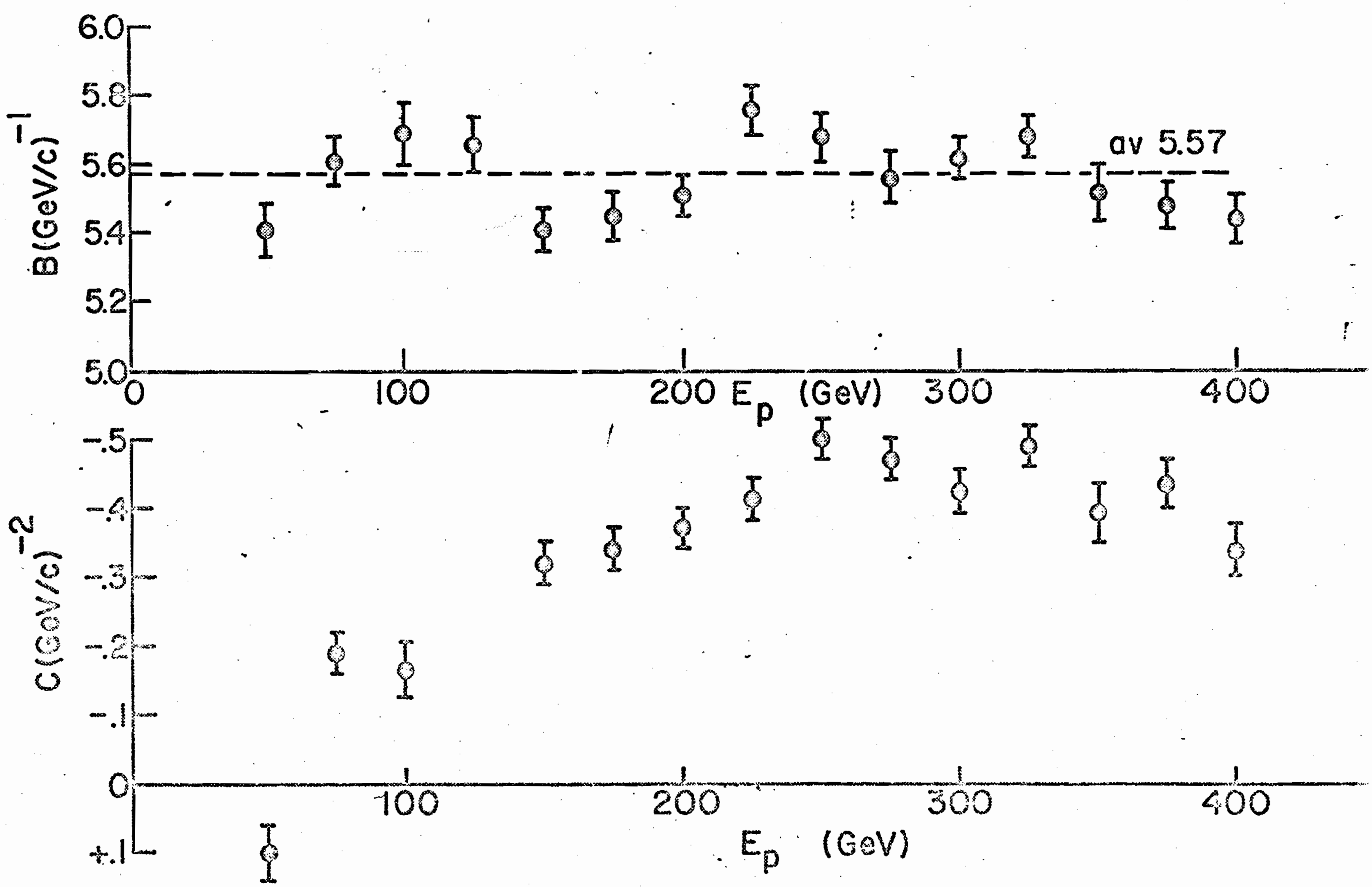

6.0
5.8
5.6
5.4
5.2
5.0
$B(GeV/c)^{-1}$
av 5.57
0
100
200
300
400
E_p (GeV)
-.5
-.4
-.3
-.2
-.1
0
+.1
$C(GeV/c)^{-2}$
100
200
300
400
E_p (GeV)

FIGURE 7

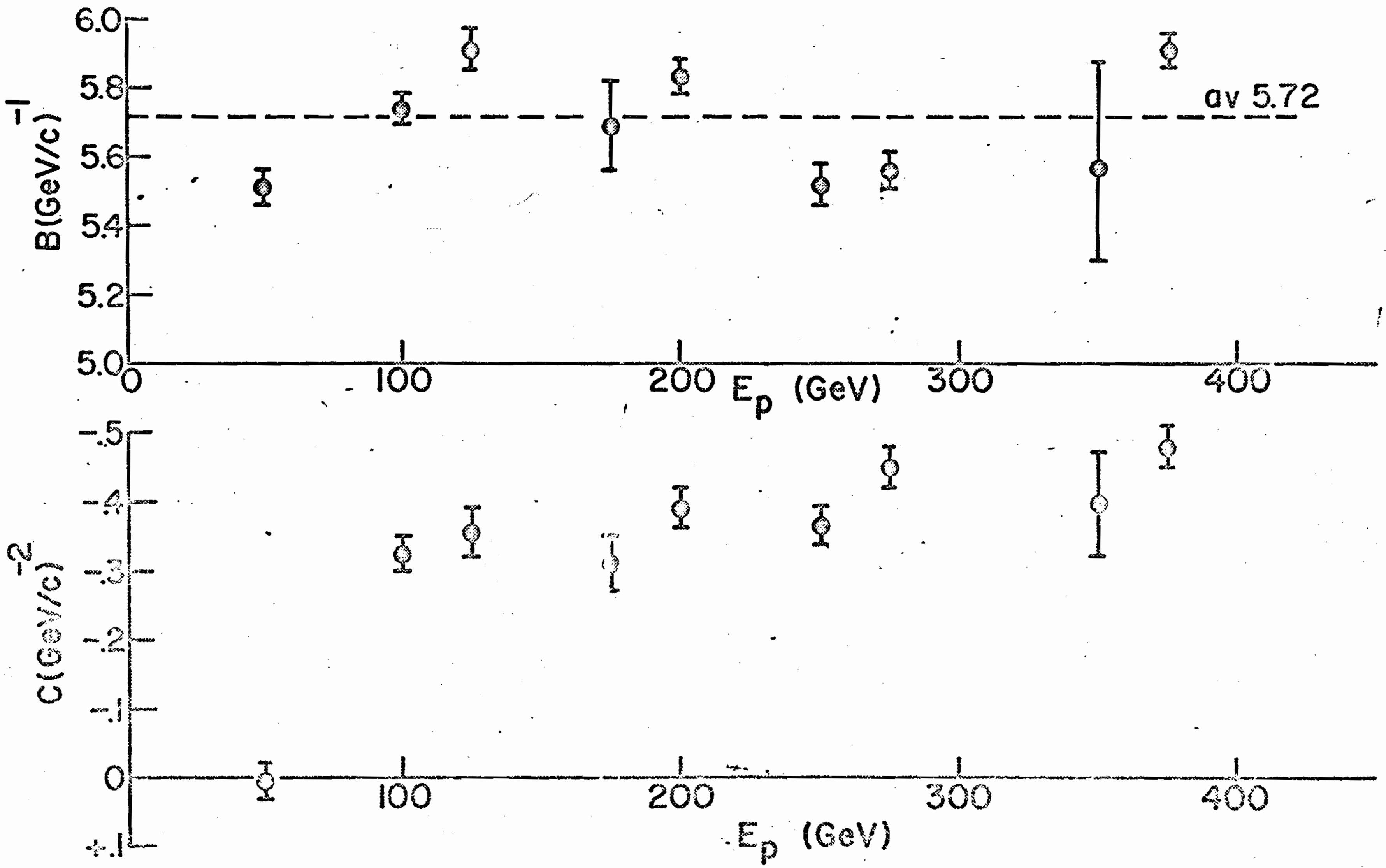

6.0
5.8
5.6
5.4
5.2
5.0
B(GeV/c)^-1
av 5.72
0
100
200
300
400
E_p (GeV)
-.5
-.4
-.3
-.2
-.1
0
+.1
C(GeV/c)^-2
100
200
300
400
E_p (GeV)

FIGURE 8

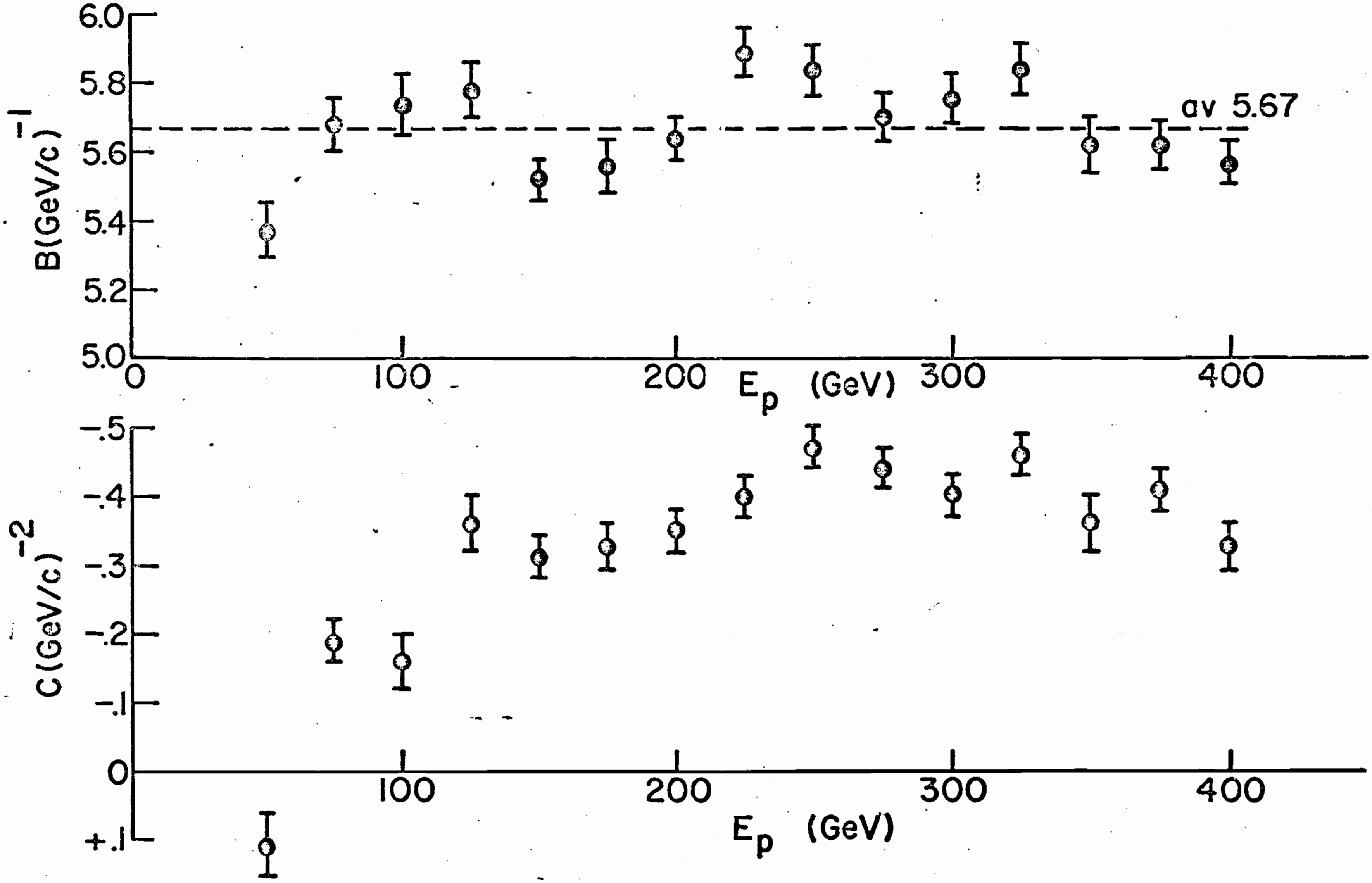

6.0
5.8
5.6
5.4
5.2
5.0
B(GeV/c)$^{-1}$
av 5.67
0
100
200
300
400
E_p (GeV)
-.5
-.4
-.3
-.2
-.1
0
+.1
C(GeV/c)$^{-2}$
100
200
300
400
E_p (GeV)

FIGURE 9